Off-axis cyclic radial shearing interferometer for measurement of centrally blocked transient wavefront

Tong Ling, Dong Liu,* Yongying Yang, Lei Sun, Chao Tian, and Yibing Shen

State Key Laboratory of Modern Optical Instrumentation, Zhejiang University, 38 Zheda Road, Hangzhou 310027, China

**Corresponding author: liudongopt@zju.edu.cn*

Received April 15, 2013; revised June 7, 2013; accepted June 10, 2013;
posted June 10, 2013 (Doc. ID 188785); published July 10, 2013

An off-axis cyclic radial shearing interferometer (OCRSI) to test a centrally blocked transient wavefront is proposed. Based on the standard cyclic radial shearing interferometer (CRSI), the OCRSI consists of a beam splitter, two folding mirrors, and a Galilean telescope. With the same but reversal tilt introduced to the two mirrors in OCRSI, the shearing interferogram can be obtained even when the central part of the test aperture is blocked. An improved wavefront retrieval method for OCRSI is employed, and a method to obtain the laterally sheared amount between the contracted and expanded beams is proposed. Numerical simulation and comparison experiments with a ZYGO GPI interferometer demonstrate that the OCRSI exhibits high precision and nice repeatability.

OCIS codes: (120.0120) Instrumentation, measurement, and metrology; (120.3180) Interferometry; (120.5050) Phase measurement.

http://dx.doi.org/10.1364/OL.38.002493

The cyclic radial shearing interferometer (CRSI) produces two contracted/expanded interfering wavefronts, traveling through the same but inverted optical path. No reference is needed because of self-interference, and vibration can be reduced by common-mode rejection [1–3]. With the spatial-carrier methods, we need only one interferogram to retrieve an asymmetrical wavefront [4,5]. Thanks to these advantages, the CRSI is widely employed in optical testing, especially online or in-process measurement [6,7]. However, the CRSI encounters problems when the center part of the aperture is blocked, for example, in transient measurement of hypersonic flow field with a model in a wind tunnel. The block will cast shadows in both contracted and expanded beams, as shown in Figs. 1(a) and 1(b), respectively. Since the radial shear is along the radial direction, the contracted beam should interfere with the central part of the expanded beam. But as is illustrated in Fig. 1(c), when the central part of the original test beam is blocked, the contracted beam will be covered by the shadow in the expanded beam partially or even entirely, and no valid interference fringe pattern can be obtained then.

In this Letter, an off-axis cyclic radial shearing interferometer (OCRSI) is proposed to solve the problem above. The OCRSI comes from a standard CRSI by slightly tilting the two folding mirrors. As illustrated in Fig. 2, when the centrally blocked test beam strikes the beam splitter (BS), it is split into two beams: after hitting the first mirror M_1, the transmitted beam is reflected to the second mirror M_2, and then travels through the Galilean telescope to be an expanded beam; meanwhile, the reflected beam goes through the telescope first, becoming a contracted beam, and travels all the way inverted. Interference happens when the transmitted and reflected beams join together again at the BS. Different from the standard CRSI, the two mirrors M_1 and M_2 have the same but reversal tilt about the vertical direction, which, as a result, makes the contracted and expanded beams deviate from the original optical axis between M_1 and M_2 but remain parallel to the optical axis in other parts of this interferometer. As a lateral shear is introduced by the tilt of M_1 and M_2, the contracted beam can eventually be moved out of the shadow of the model on the expanded beam.

As shown in Fig. 3, assume that $\boldsymbol{n}_1 = (n_{1x}, n_{1y}, n_{1z})$ and $\boldsymbol{n}_2 = (n_{2x}, n_{2y}, n_{2z})$ are the normal vectors of the mirrors M_1 and M_2, respectively; $\boldsymbol{k}_1 = (k_{1x}, k_{1y}, k_{1z})$, $\boldsymbol{k}_2 = (k_{2x}, k_{2y}, k_{2z})$, and $\boldsymbol{k}_3 = (k_{3x}, k_{3y}, k_{3z})$ are, respectively, the wave vector of the light incident on M_1 from the BS, that of the light incident on M_2 from M_1, and that of the light incident on the Galilean telescope system from M_2. According to the law of reflection, we can obtain

$$\left.\begin{aligned} \boldsymbol{k}_1 \cdot \boldsymbol{n}_1 &= -\boldsymbol{k}_2 \cdot \boldsymbol{n}_1, \\ (\boldsymbol{k}_2 - \boldsymbol{k}_1) \times \boldsymbol{n}_1 &= 0, \end{aligned}\right\}, \tag{1}$$

$$\left.\begin{aligned} \boldsymbol{k}_2 \cdot \boldsymbol{n}_2 &= -\boldsymbol{k}_3 \cdot \boldsymbol{n}_2, \\ (\boldsymbol{k}_3 - \boldsymbol{k}_2) \times \boldsymbol{n}_2 &= 0. \end{aligned}\right\}. \tag{2}$$

To form visible interference fringe patterns on the CCD, the final contracted and expanded beams exiting from the BS need to be nearly parallel to the original optical axis of the interferometer. According to the principle of reversibility of light and common-path characteristics, both $\boldsymbol{k}_1$ and $\boldsymbol{k}_3$ should also be parallel to the original optical axis, so $\boldsymbol{k}_1 = (0, 0, 1)$ and $\boldsymbol{k}_3 = (0, 1, 0)$. Substituting these values into Eqs. (1) and (2), we can obtain

$$n_{1x} = -n_{2x}, \qquad n_{1y} = n_{2z}, \qquad n_{1z} = n_{2y}. \tag{3}$$

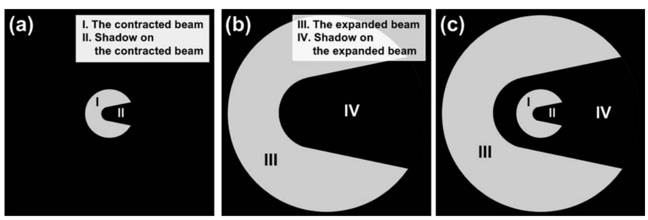

Fig. 1. Schematic diagram of the contracted and expanded beams in the CRSI with model blocking. (a) Contracted beam, (b) expanded beam, and (c) shearogram of these two beams.

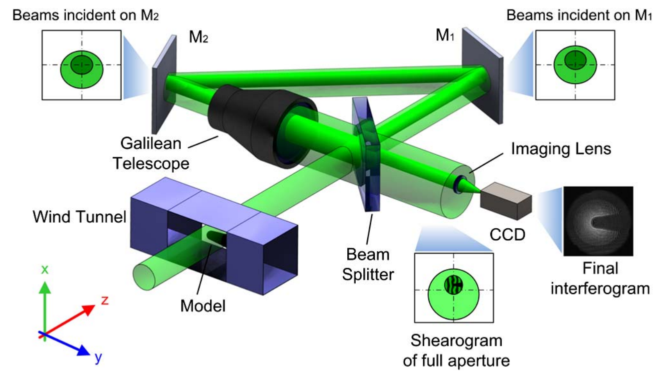

Fig. 2. Optical layout of the OCRSI used for transient hypersonic flow field testing.

Therefore, in order to make the two beams exiting the BS still parallel to the optical axis and finally interfere on the CCD, $\boldsymbol{n}_1$ and $\boldsymbol{n}_2$ should satisfy Eq. (3), which means $\theta = \theta'$. The shearogram of the shearing wavefronts exiting the BS is shown in Fig. 4, and the dotted line part shows the field-of-view (FOV) of the CCD. A coordinate system $O(u, v)$ is defined, and the laterally sheared amount between the contracted and expanded beams is $(\Delta u, \Delta v)$. If the shear ratio is defined to be s, the wavefronts of the contracted and expanded beams $W_1(u, v)$ and $W_2(u, v)$ can be described as $W(x/s, y/s)$ and $W(sx + s\Delta x, sy + s\Delta y)$, respectively. As $s\Delta x = \Delta u$ and $s\Delta y = \Delta v$ in the CCD coordinate system, the shearing wavefront can be expressed as

$$\Delta W(x/s, y/s) = W(x/s, y/s) - W(sx + \Delta u, sy + \Delta v). \quad (4)$$

Multiplying the coordinate variables x and y in Eq. (4) by $s^2, s^4, \cdots, s^{2n}$ and adding $\Delta u, \Delta u(s^2 + 1), \cdots, \Delta u \sum_{k=0}^{n-1} s^{2k}$ to variable x and $\Delta v, \Delta v(s^2 + 1), \cdots, \Delta v \sum_{k=0}^{n-1} s^{2k}$ to variable y, respectively, we can retrieve the original wavefront after some operations of summation and cancellation [8]:

$$W(x/s, y/s) = \Delta W(x/s, y/s) + \sum_{n=1}^{N} \Delta W\left[xs^{2n-1} \pm \Delta u\left(\sum_{k=0}^{n-1} s^{2k}\right), ys^{2n-1} \pm \Delta v\left(\sum_{k=0}^{n-1} s^{2k}\right)\right]. \quad (5)$$

So, given the laterally sheared amount between the centers of the contracted and expanded beams in the OCRSI, the original wavefront can be retrieved using Eq. (5). And the laterally sheared amount can be obtained with the method below. Assuming that the point $P(u, v)$

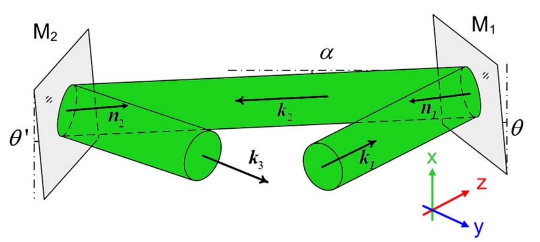

Fig. 3. Schematic diagram of the transmitted beam path reflected by M_1 and M_2 with vertical tilt.

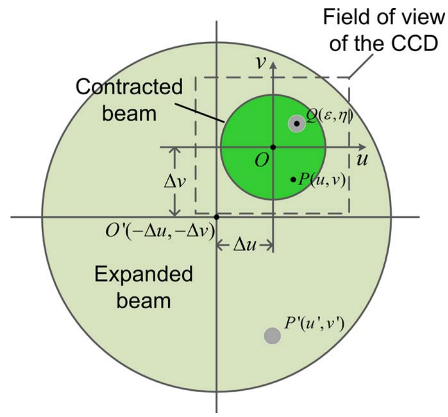

Fig. 4. Schematic diagram of the shearogram in OCRSI.

in the contracted beam and the point $P'(u', v')$ in the expanded beam in Fig. 4 correspond to the same point in the original wavefront under test, the relation between the coordinates of these two points in the OCRSI can be described in vector notation as

$$s^2\overrightarrow{O'P'} = \overrightarrow{OP}. \quad (6)$$

Before the model is set in a wind tunnel, a diaphragm with a tiny aperture is placed in front of the OCRSI, and only a small part of the light will enter the interferometer. Move the diaphragm in the x–y plane until the spots in both beams coincide with each other. The coincidence point is assumed to be $Q(\varepsilon, \eta)$, as illustrated in Fig. 4. If $P(u, v)$ and $P'(u', v')$ in Eq. (6) are replaced with the same point $Q(\varepsilon, \eta)$, we can obtain

$$s^2\overrightarrow{O'Q} = \overrightarrow{OQ}. \quad (7)$$

Substituting the coordinates of $O(0, 0)$, $O'(-\Delta u, -\Delta v)$, and $Q(\varepsilon, \eta)$ into Eq. (7), we have

$$\Delta u = (1/s^2 - 1)\varepsilon, \qquad \Delta v = (1/s^2 - 1)\eta. \quad (8)$$

As a result, with the coordinate of the coincidence point $Q(\varepsilon, \eta)$ and the shear ratio s, we can obtain the crucial laterally sheared amount $(\Delta u, \Delta v)$.

A numerical simulation is implemented to validate our method. An original wavefront of 2λ peak-to-valley (PTV) value is established using $z = 3(1-x)^2 e^{-x^2-(y+1)^2} - 10(x/5 - x^3 - y^5)e^{-x^2-y^2} - e^{-(x+1)^2-y^2}/3$, as shown in Fig. 5(a). The sampling number of the numeric array is set to 256×256, the shear ratio $s = 1{:}2$, and the laterally sheared amount is $(\Delta u, \Delta v) = (0, 128)$ pixels. The simulated radial shearing interferogram with spatial carrier is shown in Fig. 5(b). We can obtain the frequency spectrum of the interferogram by employing fast Fourier transform (FFT). After performing inverse fast Fourier transform (IFFT) of the $+1$ order spectrum, the shearing wavefront can be extracted from the interferogram [9]. With this effort, in Fig. 5(c), the original wavefront can be retrieved with Eq. (5). As shown in Fig. 5(d), the PTV and root-mean-square (RMS) of the residual error between the original and retrieved wavefronts are 0.0537λ and 0.0048λ, respectively.

An OCRSI, as illustrated in Fig. 2, with an ϕ 80 mm test aperture and a shear ratio of $s = 1{:}4$, is set up. Adjusting

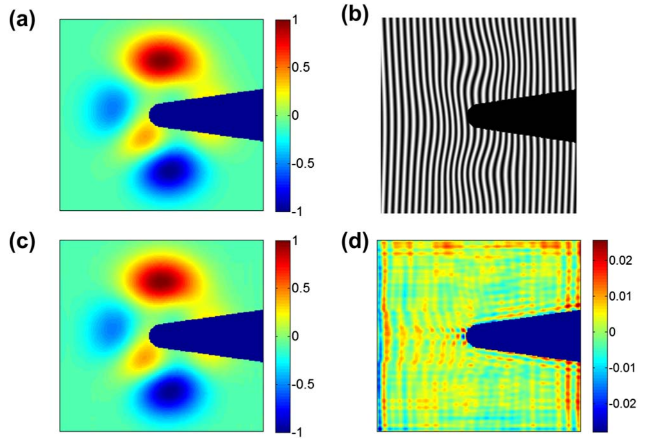

Fig. 5. Simulation results: (a) original wavefront, (b) interferogram with spatial carrier, (c) wavefront retrieved using OCRSI wavefront retrieval method, and (d) residual error between the simulation result and the original wavefront.

the vertical tilt of mirrors to the same but reversal angle, we can eventually reach a point where the contracted beam is entirely out of the shadow of model on the expanded beam. With a diaphragm, the coordinate of the coincidence point Q on CCD can be obtained as $(30, -91)$ pixels, and following Eq. (8) the laterally sheared amount $(\Delta u, \Delta v)$ equals $(450, -1365)$ pixels as our shear ratio is 1:4.

A calibration board is employed in the comparison experiment between the built OCRSI and the ZYGO GPI interferometer. In the experiment for OCRSI, the calibration board is placed in the test field where the future wind tunnel and model are supposed to lie, while for ZYGO GPI we set the calibration board between the reference flat and a good testing flat, as the principle of GPI is the Fizeau interferometer. And also, a mask acting as a model that can partially block a light beam is placed in front of the calibration board in both experiments. Though ZYGO GPI is not suitable for hypersonic testing, it is introduced to validate the precision and accuracy of our interferometer. Figures 6(a) and 6(b) show the interferogram obtained and the wavefront retrieved by our OCRSI, respectively, while ZYGO's result is shown

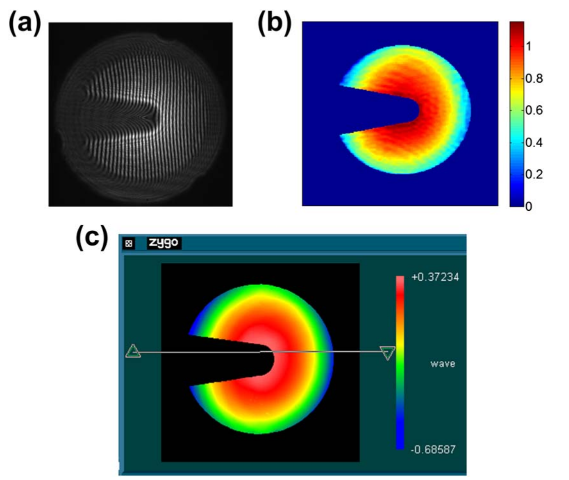

Fig. 6. Comparison experiment results between OCRSI and ZYGO GPI interferometer. (a) Interferogram obtained by OCRSI; (b) and (c) are wavefronts measured by OCRSI and ZYGO GPI, respectively.

Table 1. **Comparison Between OCRSI and ZYGO GPI**

	1	2	3	Average
Off-axis radial shearing interferometer				
P-V (λ)	1.097	1.077	1.116	1.097
RMS (λ)	0.214	0.215	0.218	0.216
ZYGO GPI interferometer				
P-V (λ)	1.058	1.097	1.069	1.075
RMS (λ)	0.218	0.221	0.218	0.219
RMS (λ) error	$\lvert 0.216 - 0.219 \rvert = 0.003$			

in Fig. 6(c). Table 1 gives the numerical results of the comparison. Compared with ZYGO, the OCRSI achieves 2.05% PTV relative error and 1.37% RMS relative error. Also, the OCRSI exhibits nice repeatability as a result of the common-path configuration.

Summarizing, we have proposed and demonstrated an OCRSI. With the same but reversal vertical tilt introduced to the two folding mirrors in the OCRSI, the contracted beam can be moved out of the model shadow on the expanded beam. As a result, the radial shearing interferogram, which is also laterally sheared, can be obtained even when the center part of the test aperture is blocked. A diaphragm with a tiny aperture is employed to get this laterally sheared amount. Taking advantage of the Fourier transform method and the improved wavefront retrieval method for OCRSI, the original transient wavefront can be obtained from a single interferogram. From both numerical simulation and experiments with a calibration board compared with the ZYGO GPI interferometer, the OCRSI exhibits high precision and nice repeatability. Different from ZYGO GPI, which requires an external reference flat and is vulnerable to environmental disturbance, the OCRSI shows good suppression over noise as a result of self-reference and common-path configuration. Since the OCRSI can obtain a steady interferogram without vibration isolation and thermostat, and can measure the transient wavefront even under partially blocked situations, it is capable of real-time high-precision measurement in a hypersonic flow field with a model in the aperture.

This work was partially supported by the National Natural Science Foundation of China (11275172), the State Key Lab. of Modern Optical Instrumentation Innovation Program (MOI201208), the "985" III: First-Class Discipline Construction Program, and the Fundamental Research Funds for the Central Universities (2013QNA5006).

References

1. P. Hariharan and D. Sen, J. Sci. Instrum. **38**, 428 (1961).
2. D. Malacara, *Optical Shop Testing* (Wiley, 1978).
3. D. Liu, Y. Yang, J. Weng, X. Zhang, B. Chen, and X. Qin, Opt. Commun. **275**, 173 (2007).
4. J. C. Xu, Q. Xu, and H. S. Pen, Appl. Opt. **47**, 5446 (2008).
5. D. Liu, Y. Yang, L. Wang, and Y. Zhuo, Appl. Opt. **46**, 8305 (2007).
6. N. Gu, L. Huang, Z. Yang, Q. Luo, and C. Rao, Opt. Lett. **36**, 3693 (2011).
7. N. I. Toto-Arellano, G. Rodriguez-Zurita, C. Meneses-Fabian, and J. F. Vazquez-Castillo, J. Opt. A **11**, 45704 (2009).
8. D. Li, F. Wen, Q. Wang, Y. Zhao, F. Li, and B. Bao, Opt. Lett. **33**, 210 (2008).
9. M. Takeda, H. Ina, and S. Kobayashi, J. Opt. Soc. Am. **72**, 156 (1982).